Impact of seawater acidification on pH at the tissue–skeleton interface and calcification in reef corals

Alexander A. Venn[a,b,1], Eric Tambutté[a,b], Michael Holcomb[a,2], Julien Laurent[a,b], Denis Allemand[a,b], and Sylvie Tambutté[a,b]

[a]Centre Scientifique de Monaco, MC-98000 Monaco, Monaco; and [b]Laboratoire Européen Associé 647 "Biosensib," Centre Scientifique de Monaco–Centre National de la Recherche Scientifique, MC-98000 Monaco, Monaco

Edited by David M. Karl, University of Hawaii, Honolulu, HI, and approved November 30, 2012 (received for review September 26, 2012)

Insight into the response of reef corals and other major marine calcifiers to ocean acidification is limited by a lack of knowledge about how seawater pH and carbonate chemistry impact the physiological processes that drive biomineralization. Ocean acidification is proposed to reduce calcification rates in corals by causing declines in internal pH at the calcifying tissue–skeleton interface where biomineralization takes place. Here, we performed an in vivo study on how partial-pressure CO_2-driven seawater acidification impacts intracellular pH in coral calcifying cells and extracellular pH in the fluid at the tissue–skeleton interface [subcalicoblastic medium (SCM)] in the coral *Stylophora pistillata*. We also measured calcification in corals grown under the same conditions of seawater acidification by measuring lateral growth of colonies and growth of aragonite crystals under the calcifying tissue. Our findings confirm that seawater acidification decreases pH of the SCM, but this decrease is gradual relative to the surrounding seawater, leading to an increasing pH gradient between the SCM and seawater. Reductions in calcification rate, both at the level of crystals and whole colonies, were only observed in our lowest pH treatment when pH was significantly depressed in the calcifying cells in addition to the SCM. Overall, our findings suggest that reef corals may mitigate the effects of seawater acidification by regulating pH in the SCM, but they also highlight the role of calcifying cell pH homeostasis in determining the response of reef corals to changes in external seawater pH and carbonate chemistry.

acid–base balance | climate change | scleractinian | carbon dioxide | acclimation

The impacts of ocean acidification on marine calcifying organisms are predicted to be varied and in many cases deleterious (1–3). Though several studies on marine calcifiers have investigated how rates of calcification respond to ocean acidification scenarios (4), comparatively few studies tackle how ocean acidification impacts the physiological mechanisms that drive calcification itself. A mechanistic understanding of calcification responses to shifts in external seawater pH and carbonate chemistry is critical to predicting how corals and other major marine calcifiers respond and potentially acclimate to ocean acidification (5).

The calcium carbonate (aragonite) skeletons of scleractinian corals make up a large component of shallow and deepwater reefs at both tropical and temperate latitudes. Corals form their skeletons by producing aragonite crystals in a fluid-filled medium called the subcalicoblastic medium (SCM) underlying the calcifying tissue [calicoblastic epithelium (CE)] (Fig. S1). The calicoblastic epithelium promotes calcification by exerting biological control over the SCM in a number of ways (reviewed in refs. 6 and 7). One important process is that the CE elevates pH in the SCM (pH_{SCM}) relative to the exterior seawater pH (8), possibly by the removal of protons via a by a Ca^{2+}ATPase (9–12). This increase in pH_{SCM} favors the conversion of bicarbonate to carbonate, elevating the saturation state of aragonite (Ω_{ar}) and enhancing its precipitation at the site of calcification (8, 9, 12–16).

As internal aragonite saturation state depends on pH_{SCM}, the ability of corals to regulate pH is anticipated to be critical to their resilience to ocean acidification (17). It has been proposed that changes in seawater pH and aragonite saturation state may be linked to decreased rates of coral calcification by lowering pH and aragonite saturation state in the SCM (18–22). Evidence comes from observations of changes in the morphology of skeletal crystals that are indicative of aragonite saturation state in the SCM (18) and also studies using boron isotope systematics (23–25). These latter studies propose corals maintain strong gradients of pH between the surrounding seawater and the SCM over large ranges of pH. However, despite intense interest in the pH of the SCM by geochemical studies, very few direct in vivo measurements of pH_{SCM} have been made. Importantly, no direct measurements of pH_{SCM} have been made in ocean acidification experiments using seawater with pH modified by elevated partial-pressure CO_2 (pCO_2).

Regulation of intracellular pH of the CE (pH_{CE}) is also anticipated to be of great importance to calcification because intracellular pH is linked to virtually all elements of cellular homeostasis, including the function of enzymes and membrane transporters (26, 27). Indeed, it has been proposed that decreases in coral calcification by ocean acidification may occur due to declines in pH_{CE} with resulting deleterious impacts on cell metabolism (15, 20, 28). However, no studies have considered the impact of ocean acidification on pH_{CE} in the calcifying cells adjoining the SCM, which are ultimately responsible for removing protons from the SCM and controlling the calcification process.

In the current study we performed an in vivo investigation into whether CO_2-driven seawater acidification causes changes in pH at the tissue–skeleton interface (pH_{SCM} and pH_{CE}) and rates of coral calcification. To achieve this we worked with *Stylophora pistillata* exposed to acidified seawater (by bubbling with CO_2) and measured pH_{SCM} and pH_{CE} using confocal imaging and the pH-sensitive probe carboxyseminaphthorhodafluor-1 (SNARF-1). To look for signs of acclimation in the responses of pH_{SCM} and pH_{CE}, we worked on two timescales: long-term (>1 y) and short-term (24-h) exposure to reduced seawater pH. We measured calcification by analyzing the growth of newly forming crystals under the calcifying tissue and also in the skeletal extension of whole colonies. We then used two models to investigate mechanisms contributing to changes of pH_{SCM} during seawater acidification. Our findings suggest that *S. pistillata* may mitigate acidification of the surrounding seawater by maintaining elevated pH and aragonite saturations in the SCM, but also suggest

Author contributions: A.A.V., E.T., D.A., and S.T. designed research; A.A.V., E.T., M.H., and J.L. performed research; A.A.V., E.T., M.H., J.L., and S.T. analyzed data; and A.A.V., M.H., D.A., and S.T. wrote the paper.

The authors declare no conflict of interest.

This article is a PNAS Direct Submission.

[1]To whom correspondence should be addressed. E-mail: alex@centrescientifique.mc.

[2]Present address: Australian Research Council Centre of Excellence in Coral Reef Studies, School of Earth and Environment and Oceans Institute, University of Western Australia, Crawley, WA 6009, Australia.

This article contains supporting information online at www.pnas.org/lookup/suppl/doi:10.1073/pnas.1216153110/-/DCSupplemental.

Table 1. Carbonate chemistry parameters in the four experimental pH treatments (means ± SD)

Treatment no.	pH_{NBS}	pH_T	Total alkalinity, μmol·kg·sw^{-1}	pCO_2, μatm	HCO_3^-, μmol·kg·sw^{-1}	CO_3^{2-}, μmol·kg·sw^{-1}	Total carbon, μmol·kg·sw^{-1}	Ωar
1	7.23 ± 0.08	7.16 ± 0.10	2,577.4 ± 60.6	4,321 ± 1383	2,474.4 ± 70.0	43.6 ± 11.6	2,638.4 ± 91.5	0.68 ± 0.18
2	7.49 ± 0.10	7.40 ± 0.16	2,544.3 ± 52.8	2,538 ± 1085	2,372.7 ± 71.0	70.7 ± 18.8	2,514.2 ± 79.5	1.10 ± 0.29
3	7.84 ± 0.09	7.76 ± 0.10	2,493.0 ± 67.0	925 ± 246	2,131.2 ± 93.2	148.3 ± 31.9	2,305.2 ± 79.3	2.30 ± 0.50
4	8.03 ± 0.07	7.93 ± 0.04	2,502.5 ± 47.1	573 ± 53	2,007.9 ± 53.5	202.6 ± 15.1	2,226.4 ± 49.3	3.14 ± 0.23

Sw, seawater; μatm, microatmospheres.

that depression of intracellular pH of the calicoblastic epithelium may be critical to the response of corals to ocean acidification.

Results

Impact of Seawater Acidification on pH at the Tissue–Skeleton Interface (pH_{SCM} and pH_{CE}). We analyzed pH_{SCM} and pH_{CE} in corals that had been exposed to four treatments of different seawater pH and carbonate chemistry (conditions in Table 1) by confocal microscopy. Samples were analyzed in a perfusion chamber, which allowed us to perfuse samples with seawater drawn from pH treatment aquaria during the analysis. We monitored pH of the perfused seawater in two positions: 5 mm (pH_{5mm}) and 100 μm ($pH_{100\mu m}$) from the surface of the sample (Fig. S1). Under optimized experimental conditions (*Materials and Methods*), these measurements verified that seawater pH in the perfusion chamber closely matched our pH treatments (Tables 1 and 2).

The first set of experiments was performed on corals that had been exposed to seawater acidification for >1 y. We determined that pH_{SCM} was significantly lower in samples from seawater pH 7.2 (treatment 1) and pH 7.4 (treatment 2) relative to our highest pH treatment, pH 8.0 (treatment 4) (Fig. 1*A*; Table 2; one-way ANOVA, $F_{3,16} = 10.30$, $P = 0.001$). The change in pH_{SCM} across the treatments was gradual, however, with respect to the surrounding seawater, leading to an increasing difference in pH between the SCM and seawater with increasing seawater acidification (Fig. 1). Analysis of the CE showed that pH_{CE} also decreased with seawater acidification, with significantly lower pH_{CE} occurring in samples maintained at pH 7.2 (treatment 1) vs. those at pH 8 (treatment 4) (Fig. 1*B*; one-way ANOVA, $F_{3,12} = 5.58$, $P < 0.05$).

Following observations made on long-term exposed corals, we also performed short-term (24-h) exposures to seawater acidification to investigate if there was a difference in the response. Measurements of pH_{SCM} and pH_{CE} revealed similar patterns to long-term exposures (Table 2). Significantly lower pH_{SCM} was measured in treatments pH 7.4 and 7.2 relative to pH 8.0 (one-way ANOVA, $F_{3,16} = 20.73$, $P < 0.001$). Significant decreases in pH_{CE} occurred in treatment pH 7.2 relative to pH 8.0 (one-way ANOVA, $F_{3,12} = 6.53$, $P < 0.05$). Direct comparison of long- and short-term data sets also indicated that the response of pH_{SCM} and pH_{CE} to the pH treatments were similar at 1 y and 24 h. Comparison of pH_{SCM} by two-way ANOVA revealed no significant differences across time and no interaction between treatment and time (two-way ANOVA, pH treatment $F_{3,29} = 31.08$, $P < 0.001$; time $F_{1,29} = 0.17$, $P > 0.05$; interaction $F_{3,29} = 1.03$, $P > 0.05$). Comparison of pH_{CE} indicated there was no significant interaction between time and treatment (two-way ANOVA, pH treatment $F_{3,24} = 11.48$, $P < 0.001$; time $F_{1,24} = 6.88$, $P < 0.05$; interaction $F_{3,24} = 0.29$, $P > 0.05$).

Impact of Seawater Acidification on Calcification. We examined the effect of seawater acidification on calcification at two scales in corals exposed for >1 y to the pH treatments—first, at the scale of newly forming crystals growing under the CE and secondly at the colony scale, by measuring increases in lateral cross-sectional area of colonies on glass slides.

Crystal growth was analyzed by measuring increases in the cross-sectional area of isolated crystals during a 4-h incubation period following a brief staining with the fluorescent dye calcein to mark time 0 (Fig. 2 *A–C*). Growth of crystals was analyzed by expressing changes in crystal the cross-sectional area as a percentage of their original size. In corals maintained at pH 8, pH 7.8, and pH 7.4, crystals increased in the cross-sectional area by 42%, 45%, and 37%, respectively (no significant difference) within the 4-h duration. In the pH 7.2 treatment, crystal growth was significantly lower than at higher pH values (10%; one-way ANOVA, $F_{3,16} = 9.92$, $P < 0.01$).

To examine whether decreases in the growth of skeletal crystals were reflected at the coral colony scale, we measured the lateral growth of corals across glass slides (Fig. 2*D*). No

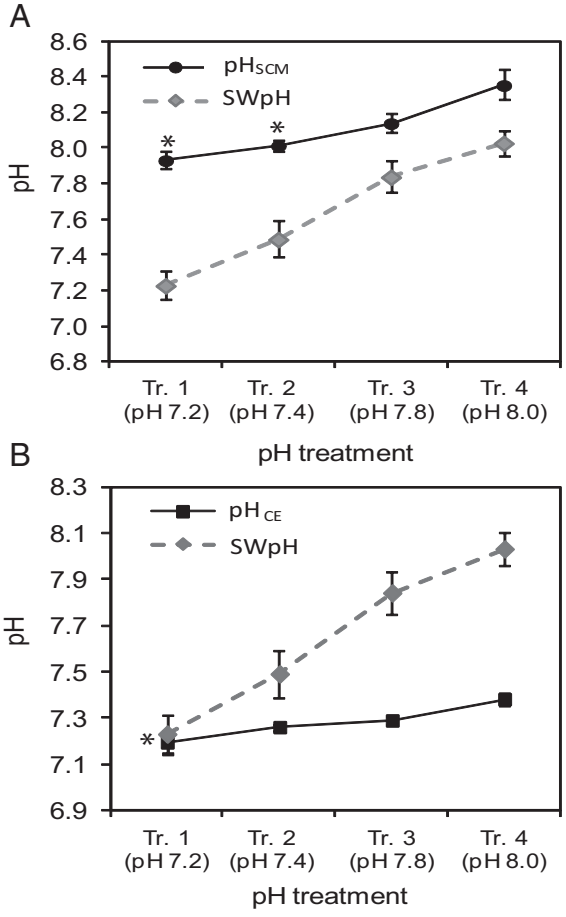

Fig. 1. The impact of CO_2-driven seawater acidification on pH at the tissue–skeleton interface in *S. pistillata* in samples exposed to experimental treatments in Table 1 for >1 y. (*A*) pH in the subcalicoblastic medium (pH_{SCM}, solid line) and pH of the treatment seawater (SWpH, dashed line). (*B*) Intracellular pH in the calicoblastic epithelium (pH_{CE}, solid line) and pH of the treatment seawater (SWpH, dashed line). Plotted values represent pH (mean ± SE, for pH_{SCM} $n = 5$ colonies, for pH_{CE} $n = 4$ colonies) determined on the NBS scale. Asterisk (*) indicates pH values significantly different to treatment 4, pH 8.0.

Table 2. Short-term (24-h) and long-term (>1 y) impacts of CO_2-driven seawater acidification on pH at the tissue–skeleton interface in *S. pistillata* in the four experiment treatments in Table 1

	Treatment 1, pH 7.2		Treatment 2, pH 7.4		Treatment 3, pH 7.8		Treatment 4, pH 8.0	
	24 h	1 y	24 h	1 y	24 h	1 y	24 h	1 y
pH_{5mm}	7.28 ± 0.07	7.19 ± 0.04	7.43 ± 0.05	7.40 ± 0.02	7.93 ± 0.07	7.79 ± 0.07	8.13 ± 0.07	8.12 ± 0.03
$pH_{100\mu m}$	7.26 ± 0.36	7.15 ± 0.10	7.41 ± 0.09	7.37 ± 0.04	7.85 ± 0.09	7.78 ± 0.10	8.03 ± 0.09	8.06 ± 0.08
pH_{CE}	7.26 ± 0.02	7.19 ± 0.05	7.32 ± 0.03	7.26 ± 0.01	7.36 ± 0.03	7.29 ± 0.02	7.41 ± 0.02	7.38 ± 0.03
pH_{SCM}	7.82 ± 0.07	7.93 ± 0.05	8.01 ± 0.06	8.02 ± 0.03	8.18 ± 0.04	8.14 ± 0.05	8.42 ± 0.04	8.36 ± 0.08

All pH values given on the NBS scale (mean ± SE; pH_{SCM}, $pH_{100\mu m}$ and pH_{5mm}: $n = 5$ colonies; pH_{CE}: $n = 4$ colonies). $pH_{100\mu m}$ and pH_{5mm}, pH in the exterior seawater at 100 μm and 5 mm from the sample; pH_{CE}, calicoblastic epithelium (calcifying cell layer); pH_{SCM}, pH in the subcalicoblastic medium (fluid at the tissue–skeleton interface).

significant differences in lateral colony growth were observed among pH treatments pH 8.0, pH 7.8, and pH 7.4, but significantly less growth was observed at the lowest pH treatment, pH 7.2 relative to pH 8 (one-way ANOVA, $F_{3,32} = 5.81$, $P < 0.01$).

Discussion

The vulnerability of calcifying organisms to ocean acidification depends partly on how changes in external seawater pH and carbonate chemistry are mitigated by the physiological processes involved in biomineralization. In corals, the capacity to regulate pH in the fluid at the tissue–skeleton interface (i.e., pH_{SCM}) and in the calcifying cells (i.e., pH_{CE}) has been widely proposed to be important in shaping calcification responses to ocean acidification (4, 15, 17, 20, 21, 28). We investigated the impact of seawater acidification on pH_{SCM} and pH_{CE} using in vivo imaging of pH in corals exposed to reduced seawater pH and elevated pCO_2 in the laboratory for long and short durations. Our experimental design included exposures to levels of acidification and elevated pCO_2 many times greater than those predicted to occur at the end of this century. Nonetheless, we observed calcification (measured by growth of skeletal crystals and whole colonies) in all our treatments, including treatment pH 7.2, where aragonite was undersaturated. This finding agrees with previous work with *S. pistillata* conducted elsewhere, where net calcification was also observed over a similar range of pH and pCO_2 (23), suggesting that *S. pistillata* may have a high tolerance to decreases in seawater pH and changes in seawater chemistry.

The results of both procedures to measure calcification (growth of crystals and whole colonies) were broadly in agreement, although the decrease in calcification at pH 7.2 was sharper when measured at the level of crystals than in whole colonies. Both crystal growth and lateral extension of colonies showed significant reductions in the lowest pH treatment (treatment 1, pH 7.2) relative to treatment 4 (pH 8.0). The inclusion of the pH 7.2 treatment in the experimental design was advantageous because it presented an opportunity to investigate pH_{CE} and pH_{SCM} in corals at a physiological tipping point, where rates of calcification significantly declined.

A second important aspect of the experimental design was that we optimized our experimental conditions and monitored pH (pH_{5mm} and $pH_{100\mu m}$) in the seawater surrounding the corals

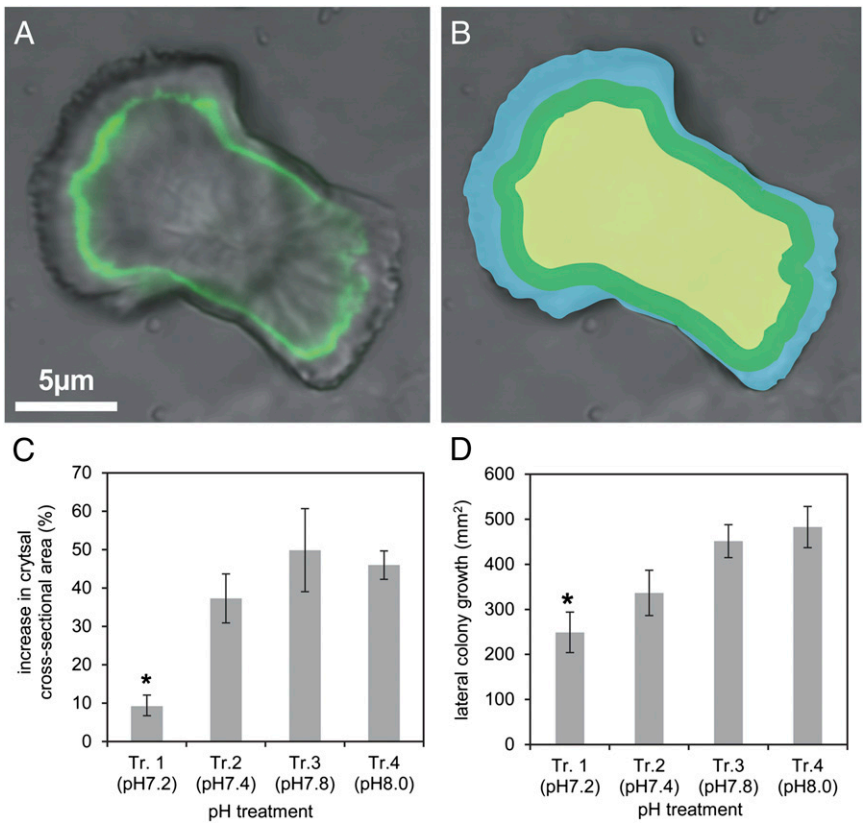

Fig. 2. (*A*) Merged confocal and transmitted light image of an aragonite crystal under the calicoblastic epithelium marked with calcein (green) at time 0 and allowed to grow for 4 h in treatment 4, pH 8.0 (treatment details given in Table 1). (*B*) The same image as *A* with the original cross-sectional area of crystal highlighted in yellow ($t = 0$) and new growth measured at $t = 4$ h highlighted in blue. Green line gives position of calcein band. (*C*) Percentage increase in a cross-sectional area of crystals in coral colonies in the four pH treatments (mean ± SE, $n = 5$ colonies). (*D*) Increase in surface area of whole coral colonies grown on glass slides for 2 mo in the four pH treatments (mean ± SE, $n = 9$ colonies). Asterisk (*) indicates mean values significantly different to treatment 4, pH 8.

during analysis to ensure that it matched our seawater treatments. Knowledge of seawater pH in the perfusion chamber was essential to ensure the pH values did not drift from treatment values during confocal analysis due to consumption and production of CO_2 by photosynthesis by the coral's symbiotic algae and respiration of both algal and coral partners in the symbiosis.

Response of pH_{SCM} to Seawater Acidification. The current study demonstrates that CO_2-driven seawater acidification causes significant declines in pH_{SCM}. Lowered pH_{SCM} under seawater acidification is anticipated to reduce rates of coral calcification, because decreases in pH_{SCM} may drive down aragonite saturation state in the SCM. It is therefore plausible that decreased pH_{SCM} lowered aragonite saturation state sufficiently in the pH 7.2 treatment to cause the significant declines in calcification observed in this treatment. An alternative explanation is that decreases in pH_{SCM} to values of pH_{SCM} 7.9 in treatment 1 (pH 7.2) disrupted other processes linked to calcification, including conformation and activity of certain secreted enzymes and proteins involved in biomineralization. Examples include *S. pistillata* secretory carbonic anhydrase (STPCA) (29), which facilitates interconversion of species of dissolved inorganic carbon, and an ortholog of the bone morphogenetic protein (BMP) (30), which may contribute to the skeletal organic matrix. Further analysis of secreted enzymes and proteins involved in coral calcification is needed to investigate this possibility, together with characterization of their behavior at different pH.

Although pH_{SCM} decreased, the observed changes in pH_{SCM} were relatively gradual with respect to the exterior seawater over the large range of seawater acidification treatments; this caused a widening difference in pH between the seawater and the SCM. Previous estimates of declining pH_{SCM} under acidification derived from boron isotope analysis of skeletons and computational models align closely with our direct measurements over a similar range of seawater pH (17). One interpretation of the results in both the present study and these previous studies is that *S. pistillata* (and perhaps other tolerant corals) mitigates seawater acidification by regulating an increasingly elevated pH_{SCM} under seawater acidification within the range of pH and carbonate chemistry tested here. Indeed, maintenance of elevated pH_{SCM} relative to the surrounding seawater may explain how several coral species continue to calcify (albeit at reduced rates) even in low pH seawater, which is undersaturated with respect to aragonite (this study and refs. 2 and 18).

Mechanisms Controlling pH_{SCM} Under Seawater Acidification. We used our pH_{SCM} values to constrain two models that explored mechanisms behind changes in pH_{SCM} at the tissue–skeleton interface. Our models considered two important processes: rates of proton removal from the SCM and rates of calcification. A third process, addition and removal of protons via the entry and exit of seawater from the SCM, remained constant in both models. Because little is known about physicochemical conditions in the SCM, our models were developed with several assumptions, which are described in Fig. S1 and *SI Materials and Methods*. Proton removal from the SCM has received attention from several previous studies that argue that pH_{SCM} is regulated by the removal of protons from the SCM by the calicoblastic cells (via a Ca^{2+}ATPase; Fig S1). Indeed, it has been proposed that corals mitigate the impacts of ocean acidification by maintaining elevated pH_{SCM} by this energy-dependant process of proton removal (17, 19). In contrast, calcification rate has received little attention as a contributing factor to pH_{SCM} under ocean acidification, although it has been considered in previous models that have investigated the composition of the SCM (31). Calcification rates are an important consideration in acid–base balance, because decreases in rates of calcification will generate fewer protons in the SCM via the calcification reaction: $Ca^{2+} + HCO_3^- = CaCO_3 + H^+$. The generation of fewer protons in the SCM will lead to a higher pH_{SCM} (if all other conditions remained the same).

In model 1 (Fig. 3*A*; Table S1) we considered a passive response in which relative energy investment in proton removal remains unchanged across our pH treatments. We thus constrained our model with constant energy investment (proton removal) and the values of pH_{SCM} that we measured in our long-term exposed corals. This model indicates that if all processes within the coral (e.g., tissue permeability, proton removal) remain constant, then a decline in external pH and aragonite saturation state leads to a decrease in calcification, although pH_{SCM} and predicted aragonite saturation states in the SCM remain elevated relative to external seawater. Importantly, model 1 demonstrates that our pH_{SCM} values can be explained with constant energy investment (i.e., no increases in proton removal rate) as long as calcification rates decrease (thus fewer protons are generated by calcification). However, although model 1 produces a general trend of declining calcification with declining external pH, the predicted trend departs from our observed trends of calcification response, particularly in the case of crystal growth, where we observed a sharp drop in calcification rate in the pH 7.2 treatment. Put more directly, model 1, which includes constant proton pumping, does not explain the threshold-like behavior of the calcification response.

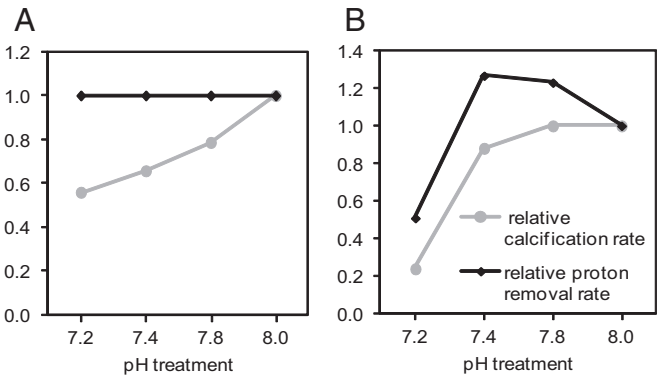

Fig. 3. Rates of proton removal and calcification in two models that explored mechanisms leading to changes in pH_{SCM}. (*A*) Model 1 assumes a fixed rate of proton removal from the subcalicoblastic medium and predicts a steady decline in calcification. (*B*) Model 2 is set with our observed relative rates of crystal growth (Fig. 2*C*) and predicts a decline in proton removal rate in treatment 1 (pH 7.2). Both models were set with our pH_{SCM} data. See *Discussion* for details.

Model 2 (Fig. 3*B*; Table S1) was therefore generated by constraining the model with the decreases in relative rates of crystal growth (shown in Fig. 2*C*) and our pH_{SCM} values, while allowing the energy investment to change to fit the observed calcification rates. Here, the model demonstrates that our observed elevated pH_{SCM} data and calcification response can be explained by variable rates of proton removal (energy investment), where proton removal rates initially increase from seawater pH treatments of 8–7.4 and then decrease at pH 7.2. One explanation of this pattern is that calicoblastic cells may initially try to compensate for the decline in the pH of the seawater entering the SCM by investing more energy into proton removal to maintain elevated pH_{SCM} and aragonite saturation state (between seawater pH treatments of 8 and 7.4). However, when seawater pH declines to 7.2, corals reduce their energy investment in proton removal, potentially reflecting an impaired functional capacity of calicoblastic cells caused by a significant depression of pH_{CE}. This explanation is just one of many possibilities, and the interplay among variations in proton removal rate, calcification rate, and the ionic composition of the SCM is an important area for future research.

Response of pH_{CE}. Declines in calcification were accompanied by a decrease in pH_{CE} in addition to reduced pH_{SCM}, highlighting a potential role of disruption to calcifying cell pH homeostasis in contributing to reduced rates of calcification. Although impacts of ocean acidification on pH_{CE} regulation were proposed early-on in ocean acidification research by previous authors (15), the response of pH_{CE} has not been investigated until the current study. Intracellular pH of the calicoblastic epithelium is anticipated to be tightly regulated because it remains at steady state in light and dark

conditions (8), and disruption to pH_{CE} has the potential to alter a wide array of cellular processes, including membrane transport, the assembly of proteins, and the activity of intracellular enzymes (26). Indeed, reductions in intracellular pH of only 0.1–0.2 pH units have been associated with reductions in cellular metabolism in other marine invertebrates (32). Because biomineralization relies on transport of molecules such as calcium and dissolved inorganic carbon, and the intracellular production and secretion of extracellular enzymes such as carbonic anhydrase (which may also be affected by changes in pH_{SCM}), changes in pH_{CE} may be expected to cause changes in calcification.

Previous work on gene expression and calcification responses in corals under ocean acidification has postulated that pH imbalance in calcifying cells occurs at a beginning of a cascade of processes, resulting in classic acidosis responses such as metabolic depression and other responses, including cytoskeletal remodeling and shifts in calcium homeostasis (33). The current study and the previous work (33) clearly highlight the need for further investigation into the role of pH_{CE} disruption in the ocean acidification response of corals. Although depression of pH_{CE} only occurred at very low seawater pH in *S. pistillata* in the current study, investigations with other, more-sensitive species may reveal change in pH_{CE} occurring at higher seawater pH and lower pCO_2.

Long-Term and Short-Term Responses of pH_{SCM} and pH_{CE}. After measuring pH_{SCM} and pH_{CE} in corals exposed to pH treatments for >1 y, we repeated our measurements in corals exposed for 24 h, to investigate whether the relatively gradual declines we observed in pH_{SCM} had arisen through long-term acclimation to seawater acidification. The observed responses in pH_{SCM} and pH_{CE} at the two timeframes were, however, very similar, suggesting that our *S. pistillata* colonies did not adjust steady-state maintenance of pH_{SCM} and pH_{CE} in response to seawater acidification over a year. The paucity of physiological pH data in cnidarians precludes comparisons with other coral species, but our data contrast with other marine invertebrates that display acid–base acclimation to altered environmental conditions within short timescales, such as bivalve molluscs, in which initial depressions in intracellular pH under decreased seawater pH of 7.3 recover to initial values after 2–8 d (34). The current data are a starting point for further investigation into the scope for acclimation to elevated pCO_2 and reduced pH in both *S. pistillata* and other reef corals, which will be essential to improving predictions of how of corals respond to changes in environmental seawater pH.

Conclusions and Future Research. The current report shows how CO_2-driven seawater acidification disrupts pH balance and calcification at the tissue–skeleton interface of a reef coral. Decreases in pH_{SCM} may have contributed to decreases in calcification rate at seawater pH 7.2 due to lowered aragonite saturation states in the SCM and potentially a less-favorable physicochemical environment in the SCM for the activity of enzymes involved in the calcification process. However, it is important to note that the changes in pH_{SCM} are small relative to changes in external seawater pH, and we observed an increasing pH gradient between the SCM and surrounding seawater. Models 1 and 2 indicate that mitigation of seawater acidification by regulation of the pH_{SCM} by proton removal and also declines in calcification rates are two processes that may have contributed to the delta pH gradient. For a better understanding of the how physicochemical conditions vary at the site of calcification under ocean acidification, additional carbonate parameters (e.g., dissolved inorganic carbon) must be measured in the SCM.

Second, we observed that significant decreases in pH_{CE} in our lowest pH treatment (pH 7.2) occur together with significant reductions in rates of calcification (at the crystal and colony scales), highlighting a potentially important role of disruption of calcifying cell pH in shaping the response of corals to seawater acidification. Our observations of decreases in pH_{CE} may be linked to the patterns of decreasing pH_{SCM}, because decreases in pH_{CE} may lead to lower rates of proton removal from the SCM under increasing seawater acidification. Future research is required to establish the role of pH_{CE} alteration in the response to ocean acidification. Until now, in contrast to the intense interest in the composition of the SCM (largely from the geochemical research community), little attention has been paid to calicoblastic cell physiology.

Future work should also build toward a whole organism-level understanding of acid–base balance in corals under ocean acidification. The description of changes in pH_{SCM} and pH_{CE} at the tissue–skeleton interface presented here are essential steps toward that goal. An organism-scale model of acid–base balance in corals under seawater acidification has recently been presented in the proton flux hypothesis (35), which proposes that decreased pH in the coral diffusive boundary layer (36, 37) inhibits calcification by limiting removal of protons from the coral. The decreasing difference in pH between the calicoblastic epithelium and the external seawater (Fig. 1*B*) observed in our study is consistent with this hypothesis, because the gradient for proton transport from the CE to seawater becomes less favorable with increasing seawater acidification. However, to achieve an organism-level understanding of acid–base balance in corals under ocean acidification, several areas of research must be tackled, including the dynamics of pH in other tissue layers and the coelenteron under seawater acidification, and also the mechanisms by which protons and other ions are transported between the seawater and the tissue–skeleton interface. Because light levels were kept constant in the current study to achieve stable values of $pH_{100\mu m}$ and pH_{5mm} during measurements, another priority area of research should concern the role of variation in photosynthetic rate of the corals symbiotic algae in shaping the response of pH_{SCM} and pH_{CE} to seawater acidification.

Last, it is important to note that in their natural setting, corals regularly experience fluctuations in multiple environmental parameters and available nutrition that may act additively or synergistically with variations in seawater pH and pCO_2 to disrupt pH regulation and calcification. Controlled laboratory studies, such as the present work, come with the caveat that that role of environmental heterogeneity is not taken into account. Thus, field-based studies and studies that incorporate multiple stressors are important to achieving a robust understanding of the effects of ocean acidification. Nevertheless, the paucity of our understanding of coral physiology means that carefully controlled laboratory studies continue to be essential to revealing the basics of how shifts in seawater carbonate chemistry and pH act on the physiological processes behind coral biomineralization. It is only with a better mechanistic perspective of the response of coral physiology to environmental change that forecasts of the future of coral reefs under ocean acidification and climate change can be improved.

Materials and Methods

Experimental Setup. Experiments were performed on 1-cm^2 microcolonies of *S. pistillata* grown laterally for 3 wk on glass coverslips according to the lateral skeleton preparative assay (38, 39) (Fig. S1*A*). Parent colonies and microcolonies of *S. pistillata* colonies were kept in four aquariums (each representing a pH treatment). Carbonate chemistry was manipulated in three of the four aquaria by bubbling with CO_2 to reduce pH to the National Bureau of Standards (NBS) target values of pH_{NBS} 7.2 (treatment 1), 7.4 (treatment 2), and 7.8 (treatment 3) (Table 1). A fourth aquarium was not bubbled with CO_2 (treatment 4, pH 8.0; Table 1). Details of the aquarium conditions (light, feeding, etc.), and the control and monitoring of aquaria carbonate chemistry are given in *SI Materials and Methods*.

Experimental Conditions for Confocal Microscopy. For live-tissue imaging, samples were transferred to a perfusion chamber (PeCon) closed with a glass lid and supplied with seawater drawn from the aquariums. The seawater pH and carbonate chemistry of the perfused seawater was checked by measuring total alkalinity and pH in the inflowing and outflowing seawater to check that carbonate chemistry did not drift away from the target values in aquariums during the period of measurement. To achieve stable pH and carbonate chemistry, we worked with samples that did not exceed 1 cm^2 in surface area, an irradiance of 170 μmol photons $m^{-2} \cdot s^{-1}$ (Philips 21V 150-W halogen bulb), and a flow rate (renewal rate of 40% per min of a 2.5-mL vol) at 25 °C. Measurement of oxygen in the perfusion chamber with a needle-type microsensor (PreSens) indicated oxygen levels also remained stable under these conditions. Stable values of pH and oxygen could not be

obtained under dark conditions (due to higher rates of net production of CO_2 and depletion of O_2), thus measurements of pH_{SCM} and pH_{CE} were restricted to the light.

Analysis of pH_{SCM} and pH_{CE}. Two timescales were investigated: long term (>1 y) and short term (24 h). Measurements were made by inverted confocal microscopy (Leica SP5) using ratiometric analysis of two forms of the dual-emission pH-sensitive dye SNARF-1 (Invitrogen) according to methods we published previously (8). For pH_{SCM}, samples were constantly perfused with seawater containing 45 μM cell-impermeable SNARF-1, which also allowed $pH_{100\mu m}$ (within 100 μm of the corals surface) and pH_{5mm} (at 5 mm from the sample) to be monitored in the seawater surrounding the sample. Samples were loaded with SNARF-1 for 10 min, after which measurements of pH_{SCM}, $pH_{100\mu m}$, and pH_{5mm} were taken during a 20-min period to check if values were stable. For measurements of pH_{CE}, the procedure involved 10 min of dye-loading by perfusion with seawater containing 10 μM cell-permeable SNARF-1-AM, followed by 20 min of seawater perfusion, during which pH_{CE} measurements were taken to check pH_{CE} was stable. Calibration of intracellular SNARF-1-AM and extracellular SNARF-1 to pH (NBS scale) were performed as described previously (8).

Measurements of Calcification. Calcification was assessed in coral samples exposed for >1 y to the seawater pH treatments by two methods: (*i*) Analysis of crystal growth on the glass coverslip and (*ii*) lateral growth of whole colonies on glass slides. For analysis of crystal growth, we worked with isolated crystals underlying the calicoblastic cells in contact with the SCM in the same region of tissue where pH_{SCM} was measured (100–150 μm from the growing edge). To mark the original size of crystals at time 0, samples were placed in a seawater solution of 160 μM calcein (Sigma) for 5 min to mark their peripheries. Calcein is a fluorescent label that is incorporated into growing calcium carbonate crystals (40). Samples were then returned to treatment aquaria in light conditions for 4 h. Confocal images and transmitted light images were then obtained of crystals at 40× magnification (excitation at 488 nm, emission capture 510–550 nm) to measure growth beyond the calcein mark at time 0. Changes in the cross-sectional area between time 0 and after 4 h were analyzed by Volocity 3D image analysis software (Perkin-Elmer) and expressed as a percentage increase of the original crystal size. We worked with crystals that ranged between 100 and 400 μm^2 in cross-sectional area, because pilot experiments showed that original size between these limits had no relationship to the extent of their growth at the four pH treatments. Furthermore, crystals of this size did not fuse with one another during the 4-h period. To analyze lateral growth of whole colonies, samples were prepared by removing apexes of 2 cm in length from parent *S. pistillata* colonies from each seawater treatment and fixing them to glass slides with cyanoacrylate glue (Loctite). Samples were returned to pH treatments and left to grow laterally for 2 mo. Initial surface area of the base of the apex and the surface area covered by lateral growth over 2 mo were measured by imaging the samples with a Leica Z16APO macroscope.

Models of Relative Rates of Proton Removal, Calcification, and SCM Carbonate Chemistry. We used our pH_{SCM} data to constrain two models. The first model is also constrained with constant rates of energy-dependant proton removal, and the second model is constrained with relative rates of calcification we observed in Fig. 2*C*. A full description of the assumptions made for the models is available in *SI Materials and Methods* and Fig. S1.

ACKNOWLEDGMENTS. We thank Natacha Segonds, Natalie Techer, Lionel Tosello, and Dominique Desgré for assistance. This research was funded by the government of the Principality of Monaco.

1. Kroeker KJ, Kordas RL, Crim RN, Singh GG (2010) Meta-analysis reveals negative yet variable effects of ocean acidification on marine organisms. *Ecol Lett* 13(11):1419–1434.
2. Rodolfo-Metalpa R, et al. (2011) Coral and mollusc resistance to ocean acidification adversely affected by warming. *Nat Clim Chang* 1(6):308–312.
3. Pandolfi JM, Connolly SR, Marshall DJ, Cohen AL (2011) Projecting coral reef futures under global warming and ocean acidification. *Science* 333(6041):418–422.
4. Ries J, Cohen A, McCorkle D (2009) Marine calcifiers exhibit mixed responses to CO_2-induced ocean acidification. *Geology* 37(12):1131–1134.
5. Weis VM, Allemand D (2009) Physiology. What determines coral health? *Science* 324(5931):1153–1155.
6. Allemand D, Tambutté É, Zoccola D, Tambutté S (2011) *Coral Reefs: An Ecosystem in Transition*, eds Dubinsky Z, Stambler N (Springer, New York), pp 119–150.
7. Tambutté S, et al. (2011) Coral biomineralization: From the gene to the environment. *J Exp Mar Biol Ecol* 408(1-2):58–78.
8. Venn A, Tambutté É, Holcomb M, Allemand D, Tambutté S (2011) Live tissue imaging shows reef corals elevate pH under their calcifying tissue relative to seawater. *PLoS ONE* 6(5):e20013.
9. Cohen AL, McConnaughey TA (2003) Geochemical perspectives on coral mineralization. *Rev Mineral Geochem* 54:151–187.
10. Ip YK, Lim ALL, Lim RWL (1991) Some properties of calcium-activated adenosine triphosphatase from the hermatypic coral *Galaxea fascicularis*. *Mar Biol* 111(2):191–197.
11. Zoccola D, et al. (2004) Molecular cloning and localization of a PMCA P-type calcium ATPase from the coral *Stylophora pistillata*. *Biochim Biophys Acta* 1663(1-2):117–126.
12. Al-Horani FA, Al-Moghrabi SM, de Beer D (2003) The mechanism of calcification and its relation to photosynthesis and respiration in the scleractinian coral *Galaxea fascicularis*. *Mar Biol* 142(3):419–426.
13. Barnes DJ (1970) Coral skeletons: An explanation of their growth and structure. *Science* 170(3964):1305–1308.
14. Constantz BR (1986) Coral skeleton construction: A physiochemically dominated process. *Palaios* 1(2):152–157.
15. Gattuso J-P, Allemand D, Frankignoulle M (1999) Photosynthesis and calcification at cellular, organismal and community levels in coral reefs: A review on interactions and control by carbonate chemistry. *Am Zool* 39(1):160–183.
16. Holcomb M, Cohen AL, Gabitov RI, Hutter JL (2009) Compositional and morphological features of aragonite precipitated experimentally from seawater and biogenically by corals. *Geochim Cosmochim Acta* 73(14):4166–4179.
17. McCulloch M, Falter J, Trotter J, Montagna P (2012) Coral resilience to ocean acidification and global warming through pH up-regulation. *Nat Clim Chang* 2(8):623–627.
18. Cohen AL, McCorkle DC, De Putron S, Gaetani GA, Rose KA (2009) Morphological and compositional changes in the skeletons of new coral recruits reared in acidified seawater: Insights into the biomineralization response to ocean acidification. *Geochem Geophys Geosyst* 10(1):1–12.
19. Cohen A, Holcomb M (2009) Why corals care about ocean acidification: Uncovering the mechanism. *Oceanography* 22(4):, 118–127.
20. Erez J, Reynaud S, Silverman J, Schneider K, Allemand D (2011) *Coral Reefs, an Ecosystem in Transition*, eds Dubinsky Z, Stambler N (Springer, New York), pp 151–176.
21. Ries JB (2011) A physicochemical framework for interpreting the biological calcification response to CO2-induced ocean acidification. *Geochim Cosmochim Acta* 75(14): 4053–4064.
22. Bates NR, Amat A, Andersson AJ (2010) Feedbacks and responses of coral calcification on the Bermuda reef system to seasonal changes in biological processes and ocean acidification. *Biogeosciences* 7(8):2509–2530.
23. Krief S, et al. (2010) Physiological and isotopic responses of scleractinian corals to ocean acidification. *Geochim Cosmochim Acta* 74(17):4988–5001.
24. Trotter J, et al. (2011) Quantifying the pH 'vital effect' in the temperate zooxanthellate coral *Cladocora caespitosa*: Validation of the boron seawater pH proxy. *Earth Planet Sci Lett* 303(3):163–173.
25. Anagnostou E, Huang K-F, You C-F, Sikes EL, Sherrell RM (2012) Evaluation of boron isotope ratio as a pH proxy in the deep sea coral *Desmophyllum dianthus*: Evidence of physiological pH adjustment. *Earth Planet Sci Lett* 349-350:251–260.
26. Busa WB, Nuccitelli R (1984) Metabolic regulation via intracellular pH. *Am J Physiol* 246(4 Pt 2):R409–R438.
27. Casey JR, Grinstein S, Orlowski J (2010) Sensors and regulators of intracellular pH. *Nat Rev Mol Cell Biol* 11(1):50–61.
28. Marubini F, Ferrier-Pagès C, Furla P, Allemand D (2008) Coral calcification responds to seawater acidification: A working hypothesis towards a physiological mechanism. *Coral Reefs* 27(3):491–499.
29. Moya A, et al. (2008) Carbonic anhydrase in the scleractinian coral *Stylophora pistillata*: Characterization, localization, and role in biomineralization. *J Biol Chem* 283(37):25475–25484.
30. Zoccola D, et al. (2009) Specific expression of BMP2/4 ortholog in biomineralizing tissues of corals and action on mouse BMP receptor. *Mar Biotechnol (NY)* 11(2): 260–269.
31. Adkins JF, Boyle EA, Curry WB, Lutringer A (2003) Stable isotopes in deep-sea corals and a new mechanism for "vital effects" *Geochim Cosmochim Acta* 67(6):1129–1143.
32. Reipschlager A, Portner HO (1996) Metabolic depression during environmental stress: The role of extracellular versus intracellular pH in *Sipunculus nudus*. *J Exp Biol* 199(8): 1801–1807.
33. Kaniewska P, et al. (2012) Major cellular and physiological impacts of ocean acidification on a reef building coral. *PLoS ONE* 7(4):e34659.
34. Michaelidis B, Ouzounis C, Paleras A, Pörtner HO (2005) Effects of long-term moderate hypercapnia on acid-base balance and growth rate in marine mussels *Mytilus galloprovincialis*. *Mar Ecol Prog Ser* 293:109–118.
35. Jokiel PL (2011) Ocean acidification and control of coral calcification by boundary layer limitation of proton flux. *Bull Mar Sci* 87(3):639–657.
36. Kühl M, Cohen Y, Dalsgaard T, Jorgensen BB, Revsbech NP (1995) Microenvironment and photosynthesis of zooxanthellae in scleractinian corals studied with microsensors for O_2, pH and light. *Mar Ecol Prog Ser* 117:159–172.
37. De Beer D, Kühl M, Stambler N, Vaki L (2000) A microsensor study of light enhanced Ca^{2+} uptake and photosynthesis in the reef-building hermatypic coral *Favia* sp. *Mar Ecol Prog Ser* 194:75–85.
38. Muscatine L, Tambutté É, Allemand D (1997) Morphology of coral desmocytes, cells that anchor the calicoblastic epithelium to the skeleton. *Coral Reefs* 16(4):205–213.
39. Raz-Bahat M, Erez J, Rinkevich B (2006) In vivo light-microscopic documentation for primary calcification processes in the hermatypic coral *Stylophora pistillata*. *Cell Tissue Res* 325(2):361–368.
40. Tambutte E, et al. (2012) Calcein labelling and electrophysiology: Insights on coral tissue permeability and calcification. *Proc R Soc Lond B Biol Sci* 279(1726):19–27.